Desalination and Water Treatment
www.deswater.com

doi: 10.5004/dwt.2018.22205

125 (2018) 222–226
September

Synthesis of rare earth Ce-doped TiO_2-SBA-15 catalyst and its photo catalytic degradation of Rhodamine B

Chunwei Shi[a,b,*], Junqiao Shao[a], Haiyang Wang[b], Qingquan Wei[b], Yili Duo[a]

[a]*Liaoning Shihua University, Fushun 113001, China, email: chunweishilnpu@126.com (C. Shi), 672217840@qq.com (J. Shao), duoll@lnpu.edu.cn (Y. Duo)*
[b]*Administration Center of the Yellow River Delta Sustainable Development Institute of Shandong Province, Dongying 257001, China, email: why@126.com (H. Wang), qqw123@163.com(Q. Wei)*

Received 10 February 2018; Accepted 17 March 2018

ABSTRACT

TiO_2 was loaded on SBA-15 mesoporous molecular sieves using the sol-gel method, and TiO_2-SBA-15 was doped with Ce via Ce $(NO_3)_3$ ion exchange. The two aspects of TiO_2 modification mentioned above were effectively combined. First, the TiO_2catalyst was supported on the mesoporous molecular sieve SBA-15 using a sol-gel method, and then TiO_2-SAB-15 was doped with Ce via ion exchange. The Ce-TiO_2-SBA-15 catalyst was characterized using XRD, FT-IR, and N_2 adsorption-desorption. The results showed that SBA-15 loaded with TiO_2 still had a highly ordered two-dimensional hexagonal structure, and the specific surface area was slightly reduced, which showed that the porous structure of SBA-15 was beneficial for the dispersion of TiO_2. The specific surface area of TiO_2-SBA-15 increased without any change in structure after doping with C_e. The photo catalytic effects of different catalysts were investigated using the photo catalytic degradation of rhodamine B as a probe reaction. The degradation rate of rhodamine B (98.4 %.) was highest with an illumination time of 120 min. The results showed that the rare earth Ce-TiO_2-SBA-15 catalyst can effectively reduce the photosynthesis of aquatic organisms after water pollution. The photo catalytic reaction was subject to first order reaction kinetics.

Keywords: Ce doping; Mesoporous molecular sieve; Photosynthesis; TiO_2; Rhodamine B; Aquatic organisms

1. Introduction

Rhodamine B is a synthetic cationic basic dye with characteristics such as high chromaticity and toxicity and low biodegradability, which can have serious impacts on water quality and can reduce photosynthesis in aquatic organisms after water becomes polluted. Furthermore, the degradation of rhodamine B is relatively difficult in water under natural conditions. Researchers have used methods such as adsorption [1] and microbial degradation [2] to solve water pollution problems. However, these methods have the disadvantages of complicated operation, high cost, and low efficiency. In recent years, a group of photo catalysts represented by TiO_2 that can utilize solar energy to catalyse the degradation of organic dyes has received wide attention [3–5]. This method has the advantages of simple operation and high activity. However, the use of this method is limited because of many shortcomings such as the easy agglomeration of TiO_2, low dispersion, low adsorption rate, large forbidden band width, low utilization rate of UV light, ease of producing holes-electron recombination centres when illuminated, and the reduction of quantum yield [6,7].

To extend the use of TiO_2, researchers have been firmly committed to the modification of TiO_2. On one hand, TiO_2 can be loaded onto supports with large specific surface area to disperse the active center and to facilitate catalyst recy-

*Corresponding author.

Presented at the 4th Annual Science and Technology Conference (Tesseract'17) at the School of Petroleum Technology, Pandit Deen Dayal Petroleum University, 10–12 November 2017, Gandhinagar, India

1944-3994 / 1944-3986

cling. On the other hand, TiO_2 can be modified via doping with metal ions, and this greatly improves the photo catalytic efficiency of TiO_2 after doping with other elements [8]. Since rare earth elements have special electronic structure ($4f^n6s^2$ or $4f^{n-1}5d6s^2$) and rich energy levels, replacing titanium ions with rare earth ions affects the band structure, the density of states, and the electronic structure of TiO_2. The absorption coefficient of TiO_2 in the visible region can be improved to some extent after doping with Ce, and the Ce doping is beneficial for improving the photo catalytic activity of TiO_2 as well [9–10].

In this work, the two aspects of TiO_2 modification mentioned above were effectively combined. First, the TiO_2 catalyst was supported on the mesoporous molecular sieve SBA-15 using a sol-gel method, and then TiO_2-SAB-15was doped with Ce vision exchange. The photo catalytic effect and kinetic reaction parameters of Ce-TiO_2-SAB-15 were investigated via the degradation of rhodamine B.

2. Experimental

2.1. Reagents

Rhodamine B, ethyl orthosilicate, tetra butyl titanate, P123, concentrated hydrochloric acid, and cerium nitrate were analytical grade and were all purchased from Shenyang No.3 Reagent Factory, China.

2.2. Instruments

A quartz photochemical reactor (Beijing Perfect light Technology Co., Ltd., coefficient) was used for photo catalytic degradation of rhodamine B. The UV-visible spectra were recorded using a TU-1900 dual-beam UV-visible spectrophotometer (Beijing Purkinje General Instrument Co., Ltd., China). A magnetic stirrer TOPOLINO (IKA) was used for stirring, and a SHZ-DIII circulating water vacuum pump (Zhengzhou Huate Instrument Equipment Co., Ltd., China) was used for controlling the temperature of water.

2.3. Preparation of the photo catalyst

2.3.1. Preparation of the mesoporous molecular sieve SBA-15

The mesoporous molecular sieve SBA-15 was prepared using a hydrothermal method as reported in the literature [11]. The white powder SBA-15 (S) was obtained after calcination at 550°C in air for 5 h.

2.3.2. TiO_2-SAB-15

0.8 mL of tetra butyl titan ate and 20 mL of absolute ethanol were placed in a 100 mL beaker, and then the pH of the solution was adjusted to 4 by adding concentrated hydrochloric acid. 1.0 g of SBA-15 powder was dispersed into the solution under magnetic stirring, and the mixture was continuously stirred in a water bath at a constant temperature for 4 h. Anhydrous ethanol was completely evaporated in a water bath at 90°C for 1 h. The obtained pale yellow solid powder was put into a muffle furnace and calcined at 500ºC for 3 h. TiO_2-SAB-15 (TS) was obtained after cooling and grinding.

2.3.3. Ce-TiO_2-SAB-15

50 mL of distilled water was put into a breaker, and 2.0 g of $Ce(NO_3)_3$ was added and dissolved. Then 2.0 g of TiO_2-SAB-15 was added, and the mixture was stirred with a magnetic stirrer for 24 h. The filtered sample was heated in an oven at 100°C for 1 h and then calcined at 500°C for 3 h in a muffle furnace. (Hereinafter, the calcined sample is denoted CTS).

2.4. Photo catalytic degradation of rhodamine B

The photo catalytic reaction experiment was carried out under illumination with a high pressure mercury lamp at a power of 125 W. The reaction volume was 60 mL, the light source was set above the reactor at the distance of about 10 cm, and the reaction was kept at constant temperature and constantly stirred magnetically. 0.1 g of the catalyst was added to 100 mL of the rhodamine B solution at an initial concentration of 15 mg/L. The reaction solution was gently stirred under dark conditions for 30 min before illuminations that the photo catalyst in the reaction solution and rhodamine B reached adsorption equilibrium. Under illumination, the same volume of supernatant was taken at the same time interval, and the photo catalyst particles in the liquid were removed via centrifugation. The supernatant samples were kept for measurements. The absorbance values were determined using spectrophotometer at the maximum absorption wavelength of rhodamine B (553 nm), and then the photo catalytic performance was evaluated and analysed. The degradation rate, R, was calculated as follows:

$$R = (1 - A_t/A_0) \times 100\ \% \quad (1)$$

where A_0 and A_t are the absorbance at the maximum absorption peak of the rhodamine B solution before and after degradation, respectively.

3. Results and discussion

3.1. XRD analysis

The XRD spectra of samples S, TS, and CTS are shown in Fig. 1.

There were three diffraction peaks in the small angle range of 0.5° ~ 2.0°, and these correspond to crystal diffractions of (100), (110), and (200) and are the characteristic diffraction peaks of typical two-dimensional hexagonal SBA-15. The positions of the diffraction peaks of TS are consistent with those of SBA-15, indicating that the structure of SBA-15 after being loaded with TiO_2 did not change and that the crystal integrity was good. After doping with Ce, the positions of the diffraction peaks did not change, the characteristic peaks of cerium species did not appear, and the intensity of the diffraction peaks decreased. This suggests that the grain size of SBA-15 decreased, which may have led to the increase in the specific surface area of CTS.

3.2. Infrared spectroscopy analysis

The infrared spectra of the three samples are shown in Fig. 2. There were obvious vibration peaks located at 807

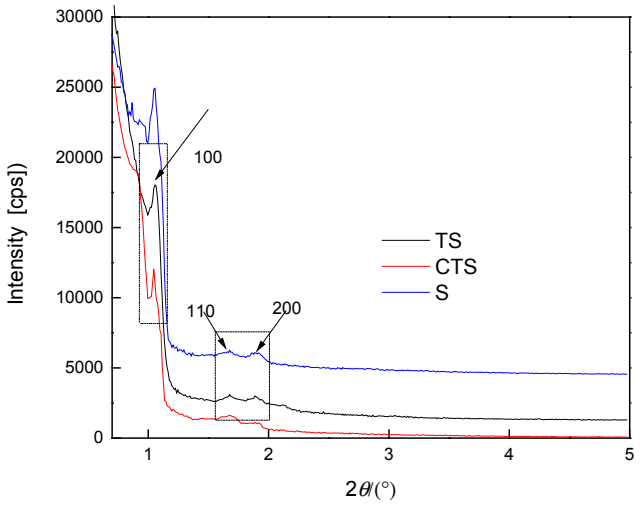

Fig. 1. SXRD patterns of S, TS and CTS.

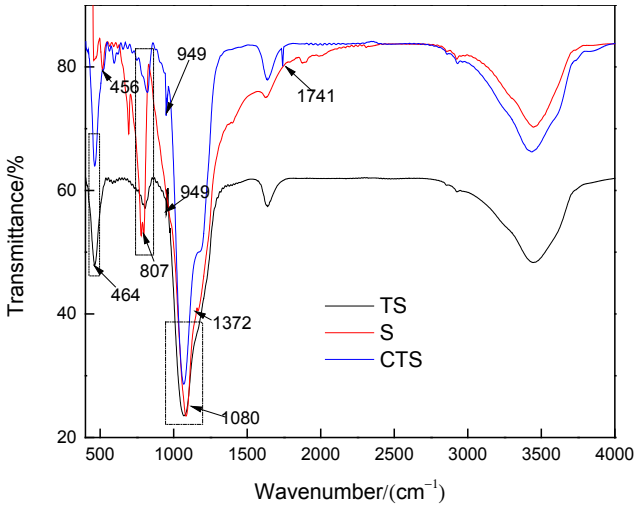

Fig. 2. Infrared spectra of S, TS and CTS.

and 1080 cm^{-1} in the curve for S, and these correspond to the symmetrical and asymmetrical stretching vibrations, respectively, of the Si–O–Si bond. The bending vibration of the Si–O–Si skeleton produced a strong absorption peak at 456 cm^{-1}. In the TS curve, the overlay of the bending vibrations (464) of the Si–O–Si and Ti–O–Ti bonds resulted in a red shift of the original peak at 456 cm^{-1}. The overlay of the Ti–O–Si and Si–OH signals caused a weak absorption peak at 949 cm^{-1} [8]. Two new absorption peaks at 1741 cm^{-1} and 1372 cm^{-1} can be attributed to the newly formed chemical bonds between the Ce ions and the surface silanols of the molecular sieve [12,13].

3.3. Specific surface area and pore size

Table 1 shows the specific surface area, pore volume, and pore size data of the samples.

The BET specific surface area of SBA-15 (615.3 m^2/g) was less than the original material (791.6 m^2/g) after the loading of TiO_2, and the BET specific surface area of the sample increased after doping with C_e, which is consistent with the prediction in Part 2.1. The pore volume remained unchanged, and the pore size decreased to 4.6 nm. Zhu et al. [14] showed that small pore size and large specific surface area improve the photo catalytic activity of crystals. Larger specific surface is beneficial for absorbing light and result in greater photo catalytic efficiency. The impact of CTS on photo catalytic activity and photo catalytic efficiency should be greater than that of TS, which can be predicted according to the specific surface area data.

Table 1
The parameters of the samples

Sample	S_{BET} /($m^2 \cdot g^{-1}$)	$V_{BJHDesorption}$ /($cm^3 \cdot g^{-1}$)	$\overline{D}_{BJHDesorption}$ /nm
S	791.6	0.80	5.6
TS	615.3	0.68	5.0
CTS	637.1	0.69	4.6

3.4. Photo catalytic performance investigation

3.4.1. Photo catalytic effects of different catalysts

Fig. 3 shows the degradation efficiencies of rhodamine B by TS and CTS. It can be seen from the figure that both TS and CTS had good degradation abilities with respect to rhodamine B at the same condition sunder simulated sunlight and that the degradation ability of CTS with respect to rhodamine B was better than that of TS, which is consistent with the prediction in Part 2.3. After 120 min of illumination, the degradation rate of rhodamine B reached 98.4%. Wang et al. [15] noted that the quantum effects of new materials doped with rare earth elements and the specific structural characteristics of such materials (such as the increase in specific surface area) are favorable for improving photo catalytic ability. El-Bahy et al. [16] found that catalytic materials exhibited stronger adsorption capacities after doping with rare earth elements. From the previous characterizations, we can see that the specific surface area of CTS was about 5% higher than that of TS with the absorption of visible light, and this was beneficial for improving the photo catalytic activity of CTS. In the meantime, it is speculated that Ti^{4+} was substituted with an appropriate amount of Ce^{3+}entering the lattice of TiO_2, and that this resulted in lattice defects and photo electron-hole separation. This allowed the effective use of hydroxyl group sand oxygen by transferring them into hydroxyl free radicals and oxygen free radicals and thereby degraded organic macromolecule contaminants and improved the photo catalytic efficiency.

Photo degradation reaction was carried out by adding 0.02 g TS catalyst in Rhodamine B solution with 80 ml concentration of 1×10^{-5} mol/L under visible light. Fig. 4 shows how the UV-Vis absorption spectrum of the solution varied with photo degradation time. The absorption peak at 553 nm corresponded to the large conjugation system composed of the benzene ring, double bond, and heterocyclic ring of rhodamine B. After 20 min of light, the absorption peak decreased significantly, and the peak at 553 nm was

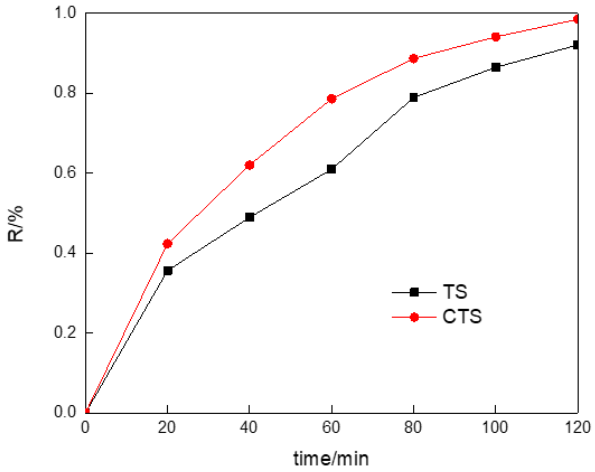

Fig. 3. Effect of different cations on the degradation of rhodamine B.

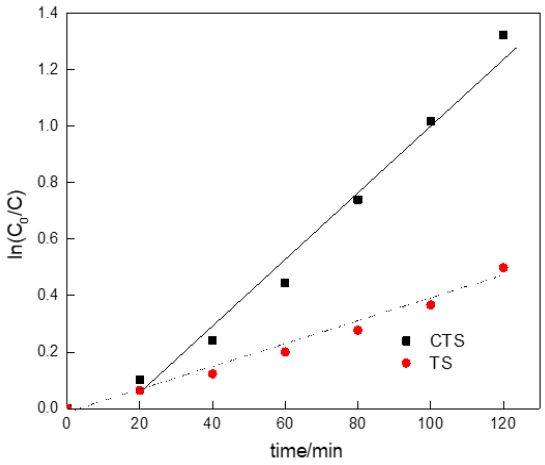

Fig. 5. The kinetic curves of degradation of methyl orange over TS and CTS.

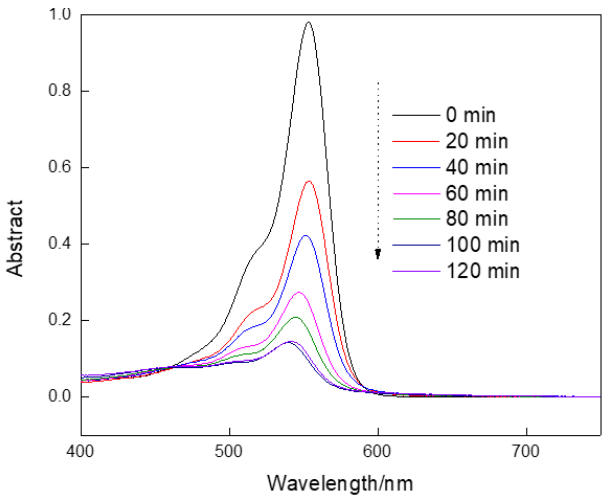

Fig. 4. UV-visible absorption spectroscopy of RhB at different degradation time.

blue shifted, which might be due to de-de-ethylation in the degradation process [16]. After 20–100 min of illumination, all of the absorption peaks were obviously reduced, the solution colour changed from its original dark red to light pink, and the absorption peak was gradually blue shifted, indicating that the damage to the aromatic ring structure of the dye occurred simultaneously with the de-methylation process [17]. After 120 min, the solution became almost colourless, which indicated the completion of the photo degradation reaction. The whole process was monitored using UV-Vis absorption spectroscopy; no new short-wavelength absorption peaks were found, indicating that there were no small organic materials produced in the degradation process.

3.4.2. Photo catalytic kinetic analysis

According to Fig. 3, the kinetics curve was obtained according to the relationship between the change in concentration (C) and time (t) in the photo catalytic degradation process of Rhodamine B in Fig. 5.

Table 2
Reaction kinetics of photo catalytic degradation of Rhodamine B

Reaction kinetic equation	$\ln(C_0/C) = 0.0036t + 0.0209$
K (min^{-1})	0.0093
$t^{1/2}$ (min)	102.12
R^2	0.9446

As shown in the figure, the photo catalytic reaction was consistent with first order kinetics and followed linear relationship according to: $\ln(C_0/C)$–t. The photo catalytic effect of CTS was better than that of TS, which was consistent with the results of the rhodamine B degradation shown in Fig. 3.

The relationship between the change of concentration (C) and the time (t) in the photo catalytic degradation of rhodamine B was fitted using the quasi-first order reaction kinetics equation: $\ln(C_0/C) = K$[18] where C_0 was 15 mg/L. Combined with the data in Fig. 5, the calculated kinetic parameters of the photo catalytic degradation reaction using CTS are shown in Table 2.

4. Conclusion

TiO_2 was loaded on an SBA-15supportand TiO_2-SBA-15 was doped with cerium ions via ion exchange. The catalyst was used in the photo catalytic degradation of rhodamine B. The results showed that Ce-TiO_2-SBA-15 had good photo catalytic activity, and the maximum degradation rate of rhodamine B was 98.4% and was obtained after 120 min of illumination. It can effectively reduce the photosynthesis of aquatic organisms after water pollution.

Acknowledgements

A part of this work was supported by the Research Fund for the Foundation of Liaoning Education Com-

mitee (L2017LQN002), the Construction of Instrument and Equipment Sharing Service Platform of Liaoning Province (2016LD0106), and the Talent Scientific Research Fund of LSHU (2016XJJ-064).

References

[1] X.L. Hao, H. Liu, G.S. Zhang, Magnetic field assisted adsorption of methyl blue onto organo-bentonite, Appl. Clay Sci., (2012) 55177–55180.
[2] K.C. Chen, J.Y. Wu, C.C. Huang, Decolorization of azo dye using PVA-immobilized microorganisms, J. Biotechnol., (2003) 101241–101252.
[3] L.M. Yun, Z.X. Yang, Z.B. Yu, Synthesis of four-angle star-like CoAl-MMO/$BiVO_4$ p–n heterojunction and its application in photo catalytic desulfurization, RSC Adv., 7 (2017) 25455-25460 .
[4] K.Z. Qi, B. Cheng , J.G. Yu, W.K. Ho, A review on TiO_2 -based Z-scheme photo catalysts, Chinese J. Catal., 38 (2017) 1936–1955.
[5] Y. Li, P.F. Wang, C.P. Huang, W.F. Yao, Q. Wu, Q.J. Xu, Synthesis and photo catalytic activity of ultra fine Ag_3PO_4 nano particles on oxygen vacated TiO_2, Appl. Catal., B 205 (2017) 489–497.
[6] M.Y. Gao, D. Jiang, D.K. Sun, Synthesis of Ag/N-TiO_2/SBA-15 photo catalysts and photo ca-catalytic reduction of CO_2 under visible light irradiation, Acta Chim. Sinica, (2014) 721092–721098.
[7] X.L. Sun, A.P. Chen, L.V. Hui, Synthesis of SBA-15/Ti/CNTs composites and their photo catalytic activities, CIESC J. (2014) 65,3718–65,3723.
[8] L. Xu, L.L. Wang, J.H. Liu. Research on preparation of iron doped TiO_2-SBA-15 catalyst and photo catalytic degradation of methyl orange, J. Dalian Univ. Technol., (2016) 5635–5641.
[9] Y. Liu, L. Yu, Z.G. Wei, Theoretical and experimental studies on photo catalytic potential of rare earth doped anatase TiO_2, Chem. J. Chinese Univ., (2013) 34434–34440.
[10] C. Zhan, F. Chen, J. Yang, Visible light responsive sulfated rare earth doped TiO_2@fumed SiO_2 composites with mesoporosity: Enhanced photo catalytic activity for methyl orange degradation, J. Hazard. Mater., 267 (2014) 88–97.
[11] L. Xu, J.H. Liu, L.L. Guo, Preparation, characterization and photo catalytic degradation of methyl orange of TiO_2-SBA-15, J. Molec. Sci., (2015) 31331–31337.
[12] D. Solís, A.L. Agudo, J. Ramírez. Hydrode sulfurization of hindered dibenzothiophenes on bifunctional NiMo catalysts supported on zeolite-alumina composites, Catal. Today, 116 (2006) 469–477.
[13] J. Wang, Y.L. Jin, Y.H. Zhou, Effect of modified HZSM-5 on the reactivity of methanol to olefins, Appl. Chem., 21 (2012) 20–24.
[14] J.F. Zhu, W. Zheng, B. He. Characterization of Fe-TiO_2 photo catalysts synthesized by hydrothermal method and their photo catalytic reactivity for photo degradation of XRG dye diluted water, J. Molec. Catal. A: Chem., 216 (2004) 35–43.
[15] C.Y. Wang, Q.J. Zhu , C.T. Gu, H.Q. Shi, D.C. Zhang, C.L.Yu, Investigation of rhodamine B photo catalytic degradation by Ce^{3+} doped Bi_2WO_6, China Environ. Sci., 35 (2015) 2682–2689.
[16] Z.M. El-Bahy, A.A. Ismail, R.M. Mohamed, Enhancement of titania by doping rare earth for photo degradation of organic dye, J. Hazard. Mater., 166 (2009) 138–143.
[17] Z. He, C. Sun, S. Yang, Photo catalytic degradation of rhodamine B by Bi_2WO_6 with electron accepting agent under microwave irradiation, J. Hazard. Mater., 162 (2009) 1477–1486.
[18] Y.N. Tang, H.G. Zhou, T. Li, Fe_3O_4/TiO_2 composite application in photo catalytic degradation of RhB, Guang dong Chem. Ind., 43 (2016) 64–68.